

One-Pot Preparation of Multicolor Polymeric Nanoparticles with High Brightness by Single Wavelength Excitation

Jian Chen,^{1,2} Fuhua Huang,¹ Hong Wang,¹ Ya Li,¹ Shengli Liu,¹ Pinggui Yi¹

¹Key Laboratory of Theoretical Organic Chemistry and Functional Molecule of Ministry of Education, Hunan Province College Key Laboratory of QSAR/QSPR, School of Chemistry and Chemical Engineering, Hunan University of Science and Technology, Xiangtan 411201, People's Republic of China

²State Key Laboratory of Chemo/Biosensing and Chemometrics, Hunan University, Changsha 410082, People's Republic of China
Correspondence to: J. Chen (E-mail: cj0066@gmail.com)

ABSTRACT: Fluorescent nanoparticles with multiplex distinct emission signatures and high brightness by a single wavelength excitation are substantially needed in multiplex bioassays and imaging. In this study, we synthesized fluorescent polymeric nanoparticles incorporated with three polymerizable organic dyes via a one-pot miniemulsion. By altering the doping ratio of three tandem dyes, the nanoparticles display abundant multiple fluorescence such as blue, cyan, green, orange, pink, red etc., together with distinguishable emission signatures under a single wavelength excitation, which were arising from the effective fluorescence resonance energy transfer (FRET) between the three energy-matched dyes. Meanwhile, a large Stokes shift (up to 250 nm) can be generated by taking place multiple FRET cascade mechanism between donor and acceptor fluorophores in nanoparticles, which also suggests broad applications in biological labeling and imaging. Moreover, these nanoparticles are uniform in size, highly bright, excellently photostable, and shown prominent longterm stability. Overall, the novel multicolor fluorescent polymeric nanoparticles augur well for their potential applications in multiplexed bioanalysis and emitting displays. © 2014 Wiley Periodicals, Inc. *J. Appl. Polym. Sci.* **2015**, *132*, 41492.

KEYWORDS: colloids; dyes/pigments; nanoparticles; nanowires and nanocrystals; optical properties

Received 27 June 2014; accepted 2 September 2014

DOI: 10.1002/app.41492

INTRODUCTION

Recently, elaboration of nanomaterials which emit multi distinguishable fluorescence signals under a single wavelength excitation have attracted considerable attention in many fields including multiplexed bioassay,¹ cell labelling,² detection of cancer cells,³ monitoring of bacteria,⁴ ratiometric sensor,⁵ and emitting displays⁶ etc. Generally, the known pathways toward fabrication of multicolor fluorescent system mainly concern quantum dots (QDs), which possess tunable emission wavelength and wide absorption bands.^{7,8} Ideally, by using QDs with six colours in 10 different intensities, a library of approximately one million optically encoded polymer microspheres were generated for parallel and high throughput analysis.¹ Moreover, QDs as multiplexed imaging probes have also revealed significant potential for *in vivo* applications. For example, QDs were evaluated for *in vivo* multiplex imaging of mouse embryonic stem cells and lymphatic basins,^{9,10} However, application of QDs as probes is often hindered by their sporadic blink, unsure long-term cytotoxicity and tedious surface functionalization.^{11,12}

Nowadays, other fascinating routes involve multicolor fluorescent nanoparticles (MFNs) assembled from materials like polymer, gold, silica and other inorganic materials have also been investigated.^{3–6,13–35} Most of these nanoparticles were designed with the encapsulation of three or more tandem organic/inorganic fluorophores, to construct a cascade fluorescence resonance energy transfer (FRET) system upon excitation.^{3–6,13–26} By varying the choice, the amount and the ratio of incorporated dyes, the MFN could reveal desired multicolor as well as fine-tuned emission spectra under a single wavelength excitation. For example, Tan et al.¹³ synthesized novel FRET-mediated multicolor silica nanoparticles, which exhibit tunable multi emissions by combination of three tandem fluorescent dyes, and further used them for simultaneous multiplexed monitoring of cancer cells and bacterial pathogens with the desired degree of sensitivity and selectivity.^{3,4} Law et al.¹⁴ prepared a series of biocompatible fluorescent polymer nanoparticles with multi distinct emission signatures by doping with combinations of four carbocyanine-based fluorophores, and used them for multiplexed imaging. Liu et al.¹⁷ reported the fabrication of

Additional Supporting Information may be found in the online version of this article.

© 2014 Wiley Periodicals, Inc.

amphiphilic and thermoresponsive diblock-copolymer-based luminescent micelles exhibiting three-state switchable multicolor fluorescence emission by external stimuli-modulated FRET process. The fluorescent nanoparticles not only exhibit multiple colors under a single wavelength excitation, but also reveal reversible photoswitch^{17,18,36} via irradiating upon UV/visible light. However, most of these reported MFNs required time-consuming synthesis and relatively strict conditions, or existed questionable dye leakage, which limited the probes application.^{15–19} In this regard, the development of versatile MFNs with not only high brightness, excellent chemical stability and photostability and adjustable emission signatures but also simplicity in synthesis with low cost is urgently desired.

To resolve some of above issues, miniemulsion polymerization technique provides a relatively promising way. Miniemulsions are small (50~500 nm) and stable oil droplets, which are dispersed in water and generally prepared by using ultrasonication devices.³⁷ Due to the negligible micellar or homogeneous nucleation during the whole polymerization process, every droplet is like an individual batch reactor. It can introduce a variety of functional materials, such as inorganic substances, magnetic nanoparticles, especially for dye molecules etc., into individual miniemulsions to form various functional polymer particles (i.e., fluorescent or magnetic polymeric nanoparticles) after polymerization.^{36,38,39} On the other hand, as comparing with other popular dye-encapsulation strategy like doping or swelling pathway,^{5,14,25} covalently incorporating dyes into nanoparticles can greatly reduce potential problems such as leakage and aggregation of dyes, which substantially improved the chemical stability and photostability of the whole MFNs system.^{13,17–19,26}

Based on the above considerations, in this work, the new multicolor fluorescent polymeric nanoparticles (MFPNs) were elaborated by covalently introducing three tandem polymerizable fluorescent dyes: 4-ethoxy-9-allyl-1,8-naphthalimide (EANI), allyl-(7-nitro-benzo[1,2,5]-oxadiazol-4-yl)-amine (NBDAA) and 10-(diethylamino)-5-oxo-5H-benzo-[a]phenoxazin-2-yl-methacrylate (NRME), into the polymeric nanoparticles via a facile one-pot miniemulsion polymerization. By varying the incorporating variety and ratio of three energy-matched dyes (EANI, NBDAA and NRME), the nanoparticles exhibit abundant multiple fluorescence such as blue, cyan, green, orange, pink, red etc., as well as distinguishable emission signals under a single wavelength excitation. Moreover, the as-prepared novel MFPNs also exhibit uniform in size, excellent photostability and long-term stability, as well as extremely high brightness. Meanwhile, seven particles that display distinct luminescence were utilized in transparent fluorescent ink for fluorescent writing. Overall, these MFPNs will be quite useful for fluorescent patterning, *in vitro* multiplexed bioassays and *in vivo* studies.

EXPERIMENTAL

Materials

The surfactant sodium dodecyl sulfate (SDS, 99%, Sigma-Aldrich), *n*-hexadecane (HD, 99%, Sigma-Aldrich), 4-bromo-1,8-naphthalic anhydride (99%, TCI Shanghai), 4-chloro-7-nitrobenzofurazan (NBD-Cl, 99%, TCI Shanghai), allylamine (99%, Aladdin), methacryloyl chloride (95%, Aladdin) was used

as received. Dichloromethane (A.R.) was washed with sulfuric acid and then distilled from CaH₂. Potassium persulfate (KPS, 99.99%, Sigma-Aldrich) was recrystallized from water and dried under vacuum. Methyl methacrylate (MMA, Sigma-Aldrich) was purified by distillation under vacuum to remove inhibitors. The water used in this work is the double-distilled water which was further purified with a Milli-Q system. Tetrahydrofuran (THF, A.R.) and Triethylamine (A.R.) were distilled over CaH₂. Petroleum ether, and other reagents were analytical reagents and used without further purification. EANI and NBDAA comonomers were achieved as described elsewhere.^{18,40–42}

Synthesis of NRME Comonomer

First, 9-Diethylamino-2-hydroxy-5H-benzo[a]phenoxazin-5-one (NROH) was synthesized in two steps following literature procedures.⁴³ Subsequently, NROH (1.2 mmol, 401 mg) and triethylamine (3 equivalent, 3.6 mmol, 548 mg) were dissolved in 50 mL of anhydrous dichloromethane, under argon equipped with a CaCl₂ moisture trap. Then methacryloyl chloride (1.5 equivalent, 1.8 mmol, 190 mg) is added to the dark-red solution. The mixture is stirred at room temperature during 24 h, until disappearance of the NROH trace on TLC. The mixture was concentrated and the residue was purified by chromatography on silica gel (ethyl acetate/petroleum ether: 1/3), affording 421 mg of product (80% yield). ¹H NMR spectrum for the product is shown in Supporting Information Figure S1 (500 MHz, DMSO-d₆, 25°C). δ (ppm): 8.26 (1H, s), 8.17 (1H, *d*), 7.61 (1H, *d*), 7.52 (1H, *d*), 6.84 (1H, *d*), 6.68 (1H, s), 6.37 (1H, *d*), 6.29 (1H, dd), 5.98 (1H, *d*), 3.51 (4H, q), 2.06 (3H, s), 1.17 (6H, *t*).

Preparation of Novel MFPNs

A mixture containing the monomer (MMA, 0.625 g) hydrophobic dyes (EANI, NBDAA and NRME, see Table I), and hydrophobe (HD, 0.038 g) was added to 10 mL water solution with emulsifier (SDS, 0.025 g) and stirred (1000 r/min) for 15 min, then, the mixture was ultrasonicated for 15 min (JY92-IIN) to obtain a stable miniemulsion. The mixture was cooled in an ice-bath during ultrasonication to avoid overheated. The resulting miniemulsion was put into a 50 mL flask equipped with a condenser, which was immersed in an oil bath with a thermostat. The polymerization was started by adding an aqueous solution of KPS (0.022 g) and preceded at 75°C for 180 min. After the polymerization, the as-prepared nanoparticle dispersions were dialyzed three times to remove uncombined dyes or monomers. Finally, the purified nanoparticles dispersions were obtained.

Characterization

¹H NMR spectra were recorded on a Bruker Avance 500 MHz NMR spectrometer. The nanoparticle diameters were determined by a Malvern Nano-ZS90 instrument and their morphology was observed with a JEM-100CXII TEM at 60 kV. UV-Vis spectra were recorded on a Shimadzu UV-2501PC spectrophotometer at room temperature (298 K). Fluorescence spectra were recorded on a Shimadzu RF-5301PC fluorescence spectrophotometer at room temperature (298 K). Fluorescence quantum yield (Φ_f) was measured on an Edinburgh FLS920 (UK) fluorescence spectrometer equipped with an integrating sphere

Table I. Spectroscopic Properties of the Three Tandem Fluorescent Dyes

Dye ^a	$\lambda_{\text{abs}}/\text{nm}$	$\lambda_{\text{em}}/\text{nm}$	$\epsilon (\times 10^{-4})/\text{L mol}^{-1} \text{ cm}^{-1}$	Φ_F^b	τ^c/ns	$B^d (\times 10^{-4})/\text{L mol}^{-1} \text{ cm}^{-1}$
EANI	363	432	1.30	0.92	7.2	1.19
NBDAA	446	511	1.90	0.94	9.8	1.79
NRME	543	605	4.40	0.90	4.7	3.96

^aRecorded in dichloromethane at 25°C.

^bObtained from Edinburgh Instruments FLS920.

^cDecay fitted with a monoexponential function ($\lambda_{\text{ex}} = 405 \text{ nm}$; for EANI, $\lambda_{\text{em}} = 432 \text{ nm}$; for NBDAA, $\lambda_{\text{em}} = 511 \text{ nm}$; for NRME, $\lambda_{\text{em}} = 605 \text{ nm}$, concentrations for all dyes in dichloromethane are 0.01 mg/mL).

^dMolecular brightness, $B = \epsilon \times \Phi_F$.

detector. Fluorescence lifetime (τ) measurements were carried out with a time correlated single photon counting (TCSPC) nanosecond fluorescence spectrometer (Edinburgh FLS920) at ambient temperature (298 K). For fluorescent dyes, data analysis was performed by simple tail fit method and fitted with a monoexponential decay function. The goodness of fit was estimated by using χ^2 values (between 1.0 and 1.2).

For multiexponential fluorescent decays (nanoparticles), no fit was attempted and the average fluorescence lifetimes were calculated by integrating the area below the decay curve as:⁴⁴

$$\langle \tau \rangle = \frac{\int_0^{\infty} tI(t) dt}{\int_0^{\infty} I(t) dt} \quad (1)$$

RESULTS AND DISCUSSION

Synthesis of Three Tandem Fluorescent Dyes

According to the principle of FRET,⁴⁵ an efficient FRET system was determined by two key factors: First, the donor's emission spectrum need to well overlap with the acceptor's absorption spectrum; then, the distance of donor–acceptor's pair should be within the effective Förster effective radius (generally, 1–10 nm). For typical fluorescence modulation systems, the distance of donor–acceptor's pair can be controlled by inserting a spacer between them or modulating their amount and ratio in size-defined nanoparticles.^{18,45} In this work, three tandem fluorophores [EANI, NBDAA, and NRME, Figure 1(a)] were elaborately synthesized to make for constructing efficient cascade

FRET system. As showed in Figure 1(b), EANI was a well-matched donor for NBDAA and partly matched donor for NRME, while NBDAA acted as both an acceptor for EANI and a donor for NRME. In addition, the spectroscopic properties of the three tandem dyes recorded in dichloromethane are given in Table I. All of the three dyes exhibited a similar Stokes shift around 60 nm, and showed a high quantum yield (Φ_F) at 0.92, 0.94, and 0.90. Furthermore, time-resolved fluorescence measurements of all dyes were made in dichloromethane. Fluorescence decays of three dyes could be fitted by a monoexponential function (Supporting Information Figures S2) and lifetimes were estimated to be 7.2, 9.4, and 4.8 ns. These results revealed the selected candidates for fabrication of FRET-mediated multicolor nanoparticles system are very appropriate.

Preparation of Novel MFPNs

To prevent possible dye leakage or aggregation, two or three fluorescent dyes (EANI, NBDAA, and NRME) were covalently encapsulated into the FRET-based multicolor nanoparticle systems via one-pot miniemulsion polymerization. Typical procedures are attached as follows. First, a solution containing the monomer (MMA), hydrophobic polymerizable dyes (EANI, NBDAA, and NRME), hydrophobes (HD), and initiator (AIBN) was dispersed into water with surfactant (SDS) to form a stable miniemulsion by ultrasonication; then, the polymerization can be achieved by increasing temperature to 75°C for 180 min, after further purification process, the as-prepared MFPNs were obtained. Certainly, this strategy can effectively enhance the

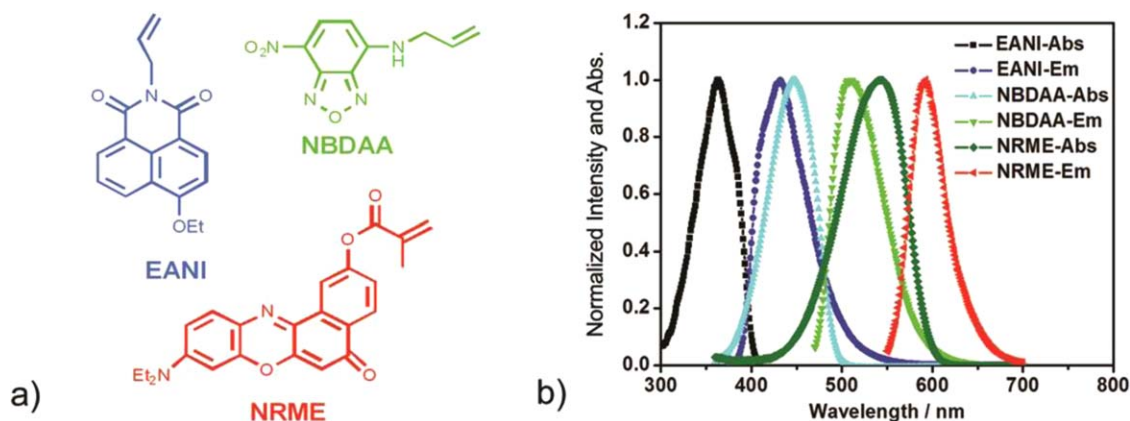
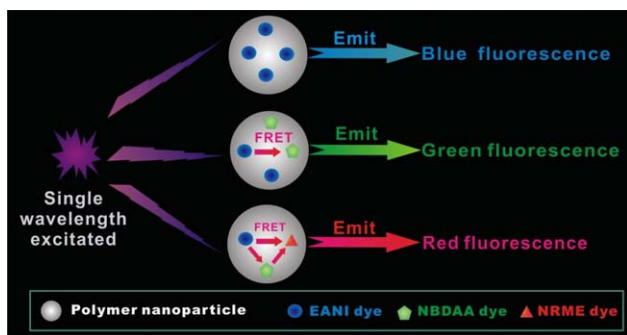


Figure 1. (a) The chemical structures of EANI, NBDAA, NRME; (b) A comparison of the normalized absorption and fluorescence emission spectra among the three fluorophores in dichloromethane. [Color figure can be viewed in the online issue, which is available at wileyonlinelibrary.com.]



Scheme 1. Schematic illustration of novel MFPNs under excitation at a single wavelength. [Color figure can be viewed in the online issue, which is available at wileyonlinelibrary.com.]

chemical stability and photostability of prepared MFPNs.³⁸ More importantly, the as-prepared fluorescent nanoparticles display abundant multicolor fluorescence under a single wavelength excitation by simply varying the choice and the feed ratio of EANI-NBDAA-NRME, as illustrated in Scheme 1.

It has been well-supported that the particle size can affect the emission property of the fluorescent nanoparticles due to the scattering light (wavelength = λ) from the particle, which will be reached a maximum value when the diameter of the particle is $\lambda/2$.³⁹ Thus, nanoparticles with a smaller size should be synthesized to reduce the scattering effect. In present work, through the typical one-step miniemulsion polymerization, nanometer-sized fluorescent polymeric particles with the average diameters of 50 nm were obtained by adjusting the amount of surfactant, monomer concentration in water, as well as the ultrasonic

power and time,^{36,37} as determined by dynamic light scattering (DLS, Table II). Table 2 also exhibits that the presence of dyes had little effect on the particle size, which was ascribed to the low amount of the feed dyes (from 0.1 to 0.7 wt %) when compared to the monomer. Figure 2(a) shows a TEM graph for a typical nanoparticle sample (NP-B1). It can be seen that most of the polymer particles of the sample were discrete and regular with diameters ranging from 40 to 55 nm, in good agreement with the size distribution determined by DLS (Supporting Information Figure S3), which indicates that the miniemulsion polymerization is a promising method to fabricate fluorescent polymeric nanoparticles with defined size.

Spectroscopic Characterization of the MFPNs

Absorption and fluorescence emission spectra of the MFPNs with two dyes incorporated are presented in Figure 3. As shown in Figure 3(a), the MFPNs appear two prominent absorption for EANI ($\lambda_{\max} = 366$ nm) and NBDAA ($\lambda_{\max} = 448$ nm) after the covalent integration of EANI and NBDAA dyes, which are close to that for EANI and NBDAA in dichloromethane, respectively [Figure 1(b) and Table I]. Figure 3(a) also displayed the absorbance of NBDAA in nanoparticles gradually increases with the addition of NBDAA dye's feed, which revealed that the loading ratio of dyes can be well controlled. In addition, the color of MFPNs also changed gradually from blue to green as showed in Figure 2(b). Furthermore, as exhibited in Figure 3(b), by varying the ratio of EANI and NBDAA in MFPNs, the fluorescence emission of the MFPNs can be correspondingly varied under a single wavelength excitation, which was attributed to the adjustable FRET efficiency between the EANI and NBDAA. Above fluorescence emission changes can also be visualized by

Table II. List of Some Data and Parameters of Various MFPNs Samples

Sample ^a	Dye feed [mg ($\times 10^{-4}$ mol)]			Size ^b (nm)	Φ_F^c	$\langle \tau \rangle^d$ (ns)	B^e ($\times 10^{-6}/L \text{ mol}^{-1} \text{ cm}^{-1}$)
	EANI	NBDAA	NRME				
NP-00	0	0	0	50.3	/	/	/
NP-A1	0.94 (3.3)	0	0	51.3	0.94	8.5	2.80
NP-A2	0	2.22 (10.0)	0	55.4	0.95	10.8	6.00
NP-A3	0	0	1.36 (3.3)	54.2	0.75	4.8	5.25
NP-B1	0.94 (3.3)	0.74 (3.3)	0	49.4	0.78	7.4	5.12
NP-B2	0.94 (3.3)	1.48 (6.6)	0	53.0	0.69	/	8.88
NP-B3	0.94 (3.3)	2.22 (10.0)	0	53.8	0.61	4.3	11.36
NP-C1	0.94 (3.3)	0.74 (3.3)	0.27 (0.7)	53.9	0.83	6.9	9.15
NP-C2	0.94 (3.3)	0.74 (3.3)	1.36 (3.3)	53.0	0.67	5.6	12.88
NP-C3	0.94 (3.3)	1.48 (6.6)	0.27 (0.7)	52.0	0.64	6.1	9.20
NP-C4	0.94 (3.3)	1.48 (6.6)	1.36 (3.3)	57.5	0.54	4.8	16.54
NP-C5	0.94 (3.3)	2.22 (10.0)	1.36 (3.3)	53.2	0.51	3.8	14.95
NP-C6	0.94 (3.3)	2.22 (10.0)	0.68 (1.7)	61.1	0.48	4.0	17.34
NP-C7	0.94 (3.3)	2.22 (10.0)	0.27 (0.7)	55.0	0.60	4.3	13.57

^a The MMA/HD/SDS/KPS feed is 0.625/0.038/0.025/0.022 g, respectively.

^b Average diameter of nanoparticles were determined from DLS data.

^c Fluorescence quantum yield was obtained from Edinburgh Instruments FLS920.

^d Average fluorescence lifetime ($\lambda_{\text{ex}} = 405$ nm, for NP-A2, $\lambda_{\text{em}} = 515$ nm, for NP-A3, $\lambda_{\text{em}} = 597$ nm, for all other samples, $\lambda_{\text{em}} = 425$ nm) calculated as eq. (1).

^e Calculation of nanoparticles brightness was shown in Supporting Information.

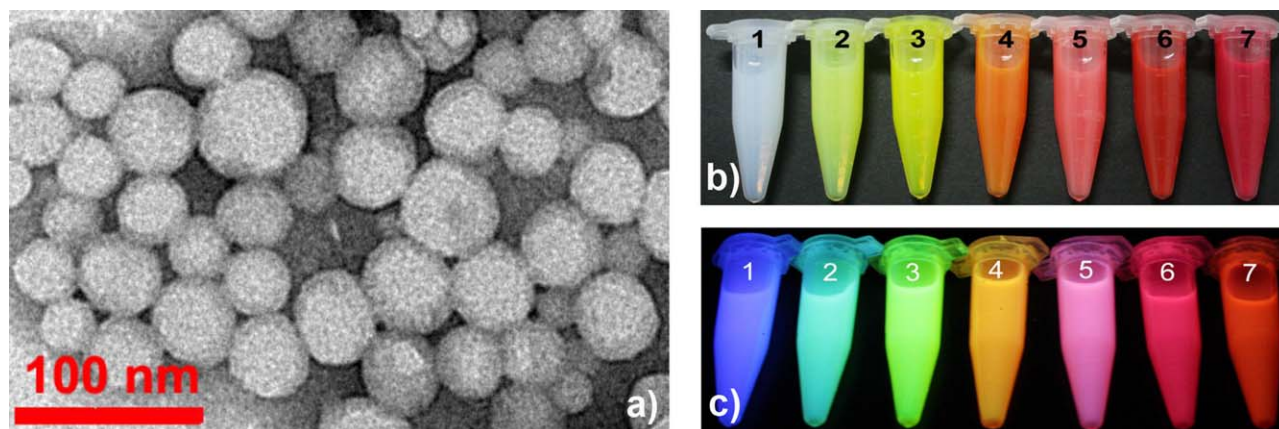


Figure 2. (a) TEM graph of one MFPNs sample (NP-B1); (b and c): photograph recorded under weight-light (b) or irradiation by a 365 nm UV portable lamp (c) for seven MFPNs samples (1: NP-A1; 2: NP-B1; 3: NP-B3; 4: NP-C7; 5: NP-C1; 6: NP-C2; 7: NP-C5). [Color figure can be viewed in the online issue, which is available at wileyonlinelibrary.com.]

the naked eye, as evidenced from the transition from blue to green [Figure 2(c), 1 to 3].

Next, the FRET cascade occurred in nanoparticles encapsulated with three tandem fluorophores (EANI, NBDAA and NRME) were investigated. NP-C1 to NP-C7 containing different ratio of EANI, NBDAA and NRME were synthesized (Table II). These particles were described as above and have similar physical properties as NP-A1 to NP-A3 and NP-B1 to NP-B3 (Table II). As exhibited in Table II, for various MFPNs containing one, two, or three dyes, fluorescence quantum yields (Φ_F) are remarkably high, which are similar to or somewhat higher than those of reported fluorescent nanoparticles with high brightness or semiconducting QDs.^{2,29,46–48} The successful encapsulations of three dyes were further confirmed by absorbance [Figure 4(a)]. Because of FRET cascade's protocol, upon excitation at 385 nm, the 597 nm emission of MFPNs with three dyes loading (Samples NP-C2, NP-C4, and NP-C5) exhibited ~ 5 to 6

times higher than the nanoparticles with only the NRME (Sample NP-A3), when the feed of NRME at the same value. In addition, most of the MFPNs showed three distinct emission peaks at 425, 515, and 597 nm [Figure 4(b–d)]. Meanwhile, the ratio of three emission peaks can be well tuned by changing the feed ratio of three dyes. For example, the MFPNs with the same feed amount of EANI and NRME, and increasing feed amount of NBDAA [Figure 4(b–c) and Table II], the emission peak of EANI decreased dramatically, while the peak of NBDAA and NRME increased slowly. At the same feed ratio of EANI and NBDAA for the MFPNs, the adding amount of NRME resulted in the relatively enhanced emission signal of NRME when compared with other two emission peaks [Figure 4(d) and Table II]. Moreover, it is worthy to note that the Stokes shift of our particles (up to 250 nm, NP-C5) was larger than other platforms with a similar design,^{13,15} which indicated that the as-prepared MFPNs possess very broad controllable emission range, so as to

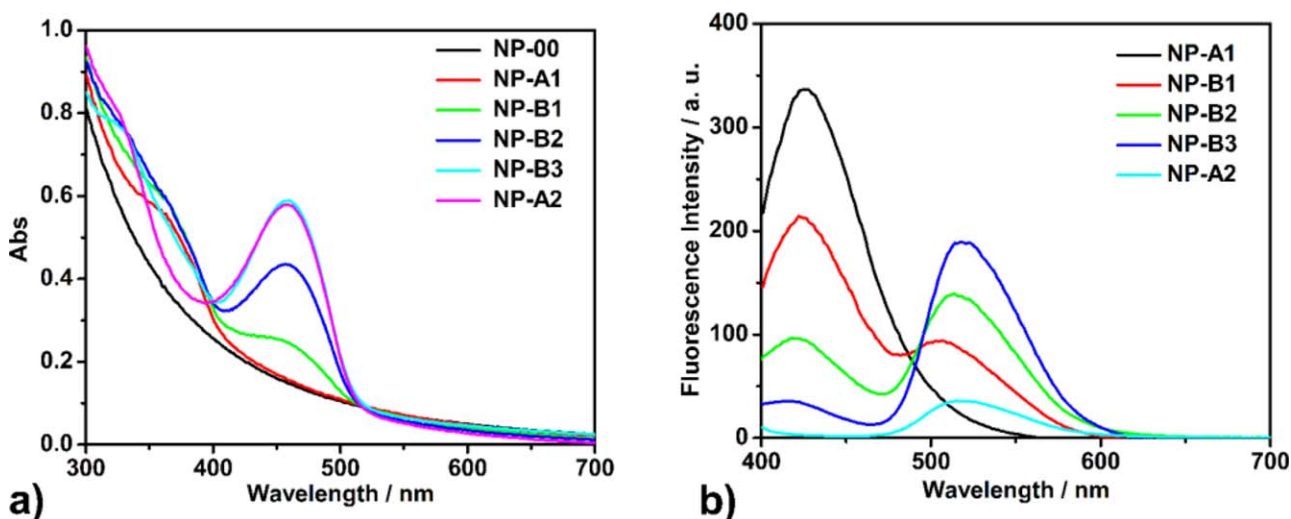


Figure 3. (a) Absorption spectral of blank polymeric nanoparticles, NP-00 and other MFPNs samples as NP-A1, NP-B1, NP-B2, NP-B3, NP-A2 (see Table I). (b) Fluorescence emission spectral of MFPNs samples as NP-A1, NP-B1, NP-B2, NP-B3, NP-A2 (see Table I, λ_{ex} =385 nm). [Color figure can be viewed in the online issue, which is available at wileyonlinelibrary.com.]

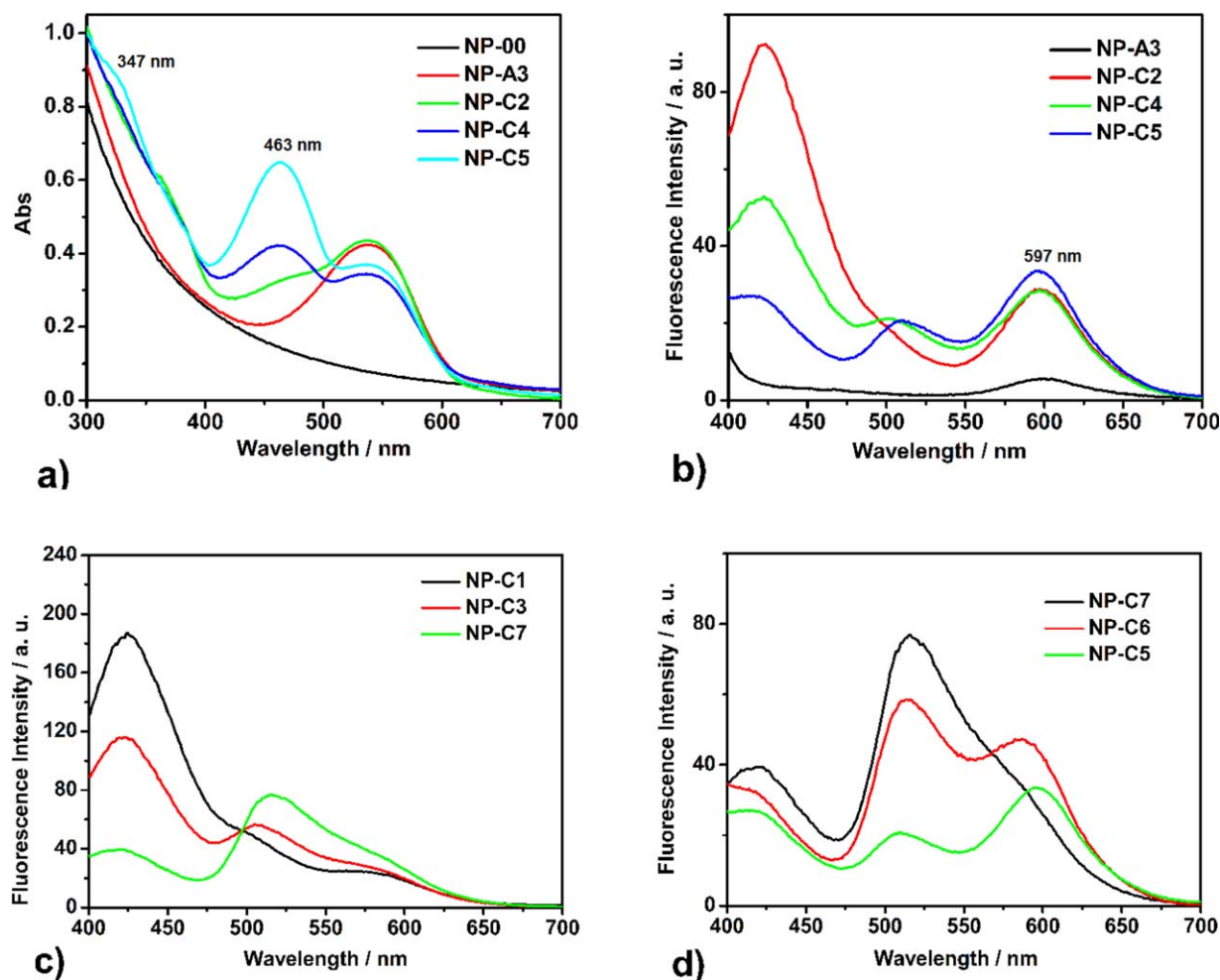


Figure 4. (a) Absorption spectral of blank polymeric nanoparticles sample NP-00 and MFPNs samples as NP-A3, NP-C2, NP-C4, NP-C5; (b) Fluorescence emission spectral of MFPNs samples as NP-A3, NP-C2, NP-C4, NP-C5; (c) Fluorescence emission spectral of MFPNs samples as NP-C1, NP-C3, NP-C7; (d) Fluorescence emission spectral of MFPNs samples as NP-C7, NP-C6, NP-C5 ($\lambda_{\text{ex}} = 385 \text{ nm}$). [Color figure can be viewed in the online issue, which is available at wileyonlinelibrary.com.]

nearly overlap the whole visible light region. Similarly, the above fluorescence emission variations can also be identified by the naked eye, as showed in Figure 2(c) (from 4 to 7).

Fluorescence decay curves (Figure 5) were achieved using the TCSPC technique, and excited-state lifetimes were extracted from the kinetics traces using custom software. The average fluorescent lifetime results of MFPNs samples are listed in Table II. The lifetimes of EANI, NBDAA and NRME-contained nanoparticles were determined to be 8.5, 10.8, and 4.8 ns, respectively, which were closed to those of selected fluorescent dyes in dichloromethane. It indicated that the selected hydrophobic fluorescent dyes have been resided in a low polarity polymeric matrix, which was analogical to dichloromethane. However, as exhibited in Figure 5(a), when fixing the EANI feed in nanoparticles, and increasing the second dye as NBDAA, the MFPNs samples, like NP-B1 and NP-B3 display much shorter lifetimes at 425 nm than that of nanoparticles with only EANI dye, significantly indicated the existing FRET process between the EANI and NBDAA; and with the adding of another dye as NRME, the lifetime of MFPNs sample like NP-C5 at 425 nm

continue to decrease a few, which is also attributed to the possible FRET between EANI and NRME. Moreover, evidence about the efficient FRET between NBDAA and NRME can also be revealed by comparing the fluorescence decay curves at 515 nm between MFPNs sample NP-B3 and NP-C5, as showed in Figure 5(b). The estimated average lifetimes of two samples are 11.0 and 5.3 ns, respectively.

For ultrahigh resolution fluorescence imaging, as well as flow cytometry, a valuable feature of fluorescent probes is the fluorescence brightness.^{23,29} The nanoparticle brightness (B) can be evaluated from reported literature elsewhere (the detailed calculation process was shown in supporting information),⁴⁶ and have been shown in Table II. In the this study, brightness values of all MFPNs samples were varied from 2.80×10^6 to $1.73 \times 10^7 \text{ cm}^{-1} \text{ mol}^{-1} \text{ L}$ (Table II), which were much higher than the selected fluorescent dyes as listed in Table I. For comparison, nanoparticle containing the optimal ratio of three dyes (NP-C6) possesses the best brightness as $1.73 \times 10^7 \text{ cm}^{-1} \text{ mol}^{-1} \text{ L}$, which is therefore ca. 29–290 times brighter than those well-known QDs with emission in the range of 370–750 nm, which

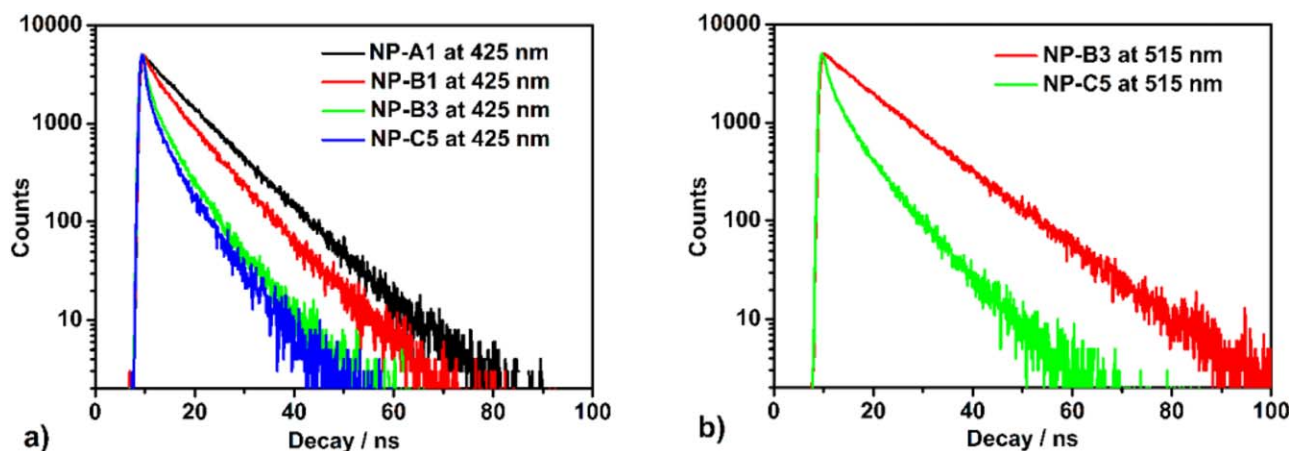


Figure 5. (a) Fluorescence decay curves of MFPNs samples as NP-A1, NP-B1, NP-B3, NP-C5 at 425 nm ($\lambda_{\text{ex}} = 405$ nm, see Table II). (b) Fluorescence decay curves of MFPNs samples as NP-B3, NP-C5 at 515 nm ($\lambda_{\text{ex}} = 405$ nm). [Color figure can be viewed in the online issue, which is available at wileyonlinelibrary.com.]

were made of CdSe, CdS, or CdTe, and have a brightness between 6×10^4 and $6 \times 10^5 \text{ cm}^{-1} \text{ mol}^{-1} \text{ L}$.⁴⁷ Meanwhile, it is also several to 10 times brighter than other reported fluorescent organic polymeric nanoparticles.⁴⁸

The photostability of MFPNs is of crucial importance for many emitting devices and fluorescence-based imaging applications, particularly for long-term imaging and tracking experiments.²⁹ Under a continuous 365 nm UV portable lamp (ZF-7A) illumination, the effect of irradiation time on the fluorescence intensity of typical MFPNs sample (NP-A2, Table II) is given in Figure 6. There is a little (<7%) decrease of fluorescence intensity within the experimental irradiation time (90 min), and after 40 min UV irradiation, the fluorescence intensity of nanoparticle dispersion seldom changes even after longer time illumination. These data establish that the MFPNs possess excellent photostability.

In addition, the long-term fluorescence stability of the typical MFPNs sample was also investigated. For this experiment, the

diluted sample was sealed in a vessel and stored in the dark under room temperature. Then an aliquot was extracted out for fluorescence intensity measurement. As displayed in Figure 7, the fluorescence intensity of the dispersions altered slightly even after storing for 42 days, indicating prominent long-term photostability in this MFPNs system. Moreover, it is known that the fluorescence intensity of dyes is significantly affected by their environment. Our previous result showed the hydrophobic dyes like NBDAA often exhibited prominent fluorescence intensity in PMMA nanoparticles, while displayed very weak fluorescence intensity in aqueous phase.¹⁸ If the dyes were transferred from the hydrophobic nanoparticles to the aqueous phase, their fluorescence intensity should decrease dramatically. Therefore, the result showed in Figure 7 also indicated the negligible dye leakage of as-prepared MFPNs. In addition, the similar result can be found in other MFPNs sample containing two dyes (Supporting Information Figure S4). These results demonstrate that the MFPNs could be invoked as promising candidates for long-term imaging or tracking.

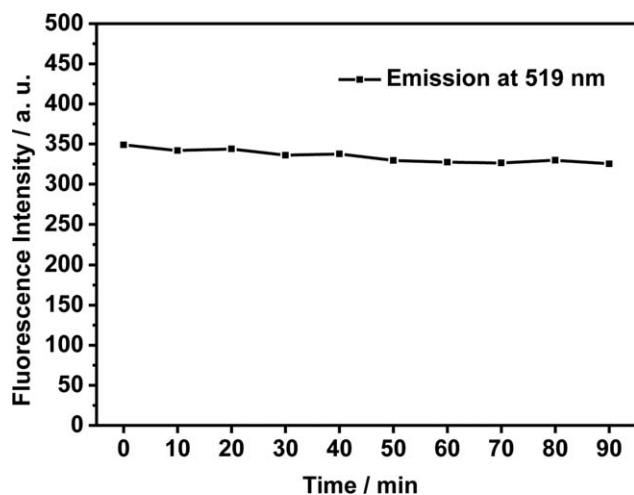


Figure 6. Fluorescence intensity changes of MFPNs sample NP-A2 under a continuous 365 nm UV lamp irradiation ($\lambda_{\text{ex}} = 490$ nm).

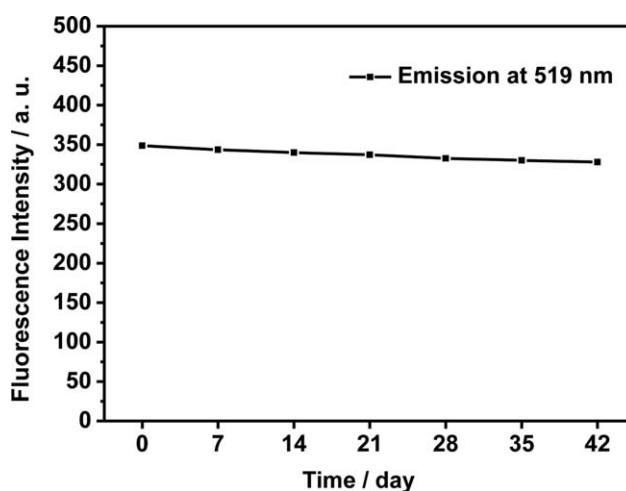


Figure 7. Fluorescence long-term photostability of MFPNs sample NP-A2 under ambient temperature and kept in the dark ($\lambda_{\text{ex}} = 490$ nm).



Figure 8. (a) Multicolor fluorescent pens obtained via using different MFPNs inks (1: NP-A1; 2: NP-B1; 3: NP-B3; 4: NP-C7; 5: NP-C1; 6: NP-C2; 7: NP-C5). (b) Photograph recorded of fluorescent pens illuminated by a portable UV lamp. (c) Photograph recorded of multicolor numbers and letters via writing on paper via different pens (from 1 to 7, or A to G) (illuminated by a portable UV lamp). [Color figure can be viewed in the online issue, which is available at wileyonlinelibrary.com.]

To make use of the high fluorescence brightness and excellent water-dispersible property, the MFPNs were utilized in fluorescent inks for special writing. Various aqueous MFPN dispersions (ca. 5 wt %) were injected into seven vacant refills to manufacture novel multicolor fluorescent pens [Figure 8(a)]. As showed in Figure 8(b), seven pens emitted intense multicolor fluorescence from blue to red under a portable 365 nm UV lamp illumination. A commercially available paper upon which the MFPNs adhered well (the paper showed no background UV fluorescence) was selected as the writing paper. After simple writing by different pens and under a 365 nm UV lamp illuminations, visible numbers, and letters with different luminescence could be easily observed [Figure 3(c)]. In this case, inks with different MFPNs dispersions could serve as separate colors for complex multicolor writing or printing [Figure 8(c)].

CONCLUSIONS

In conclusion, the novel MFPNs were synthesized via a facile one-pot miniemulsion polymerization by covalently incorporating three elaborated fluorescent dyes: EANI, NBDAA, and NRME. Within the modulation of FRET, the nanoparticles display abundant multiple emission from blue to red under a single wavelength excitation by simply changing the variety and ratio of three selected dyes. Moreover, the MFPNs also show uniform in size, extremely high brightness, appropriate fluorescent lifetimes, excellent photostability and long-term stability (>42 days). In addition, in order to reveal the applications, the MFPNs that display distinct luminescence were used as fluorescent ink for special writing. Overall, incorporation of the merits of one-pot miniemulsion polymerization techniques, we believe

that these novel MFPNs platforms, will be very useful for complex fluorescent patterning, and have far reaching potential for *in vitro* multiplexed bioassays and *in vivo* studies, when used in combination with multispectral imaging.

ACKNOWLEDGMENTS

This work was supported by National Natural Science Foundation of China (Project No. 51373002, 51003026, 21172066), Scientific Research Fund of Hunan Provincial Education Department (Project No. 12B041), Scientific Research Foundation for the Returned Overseas Chinese Scholars, State Education Ministry, Graduate Innovation Fund of Hunan University of Science and Technology (Project No. S120026), Open Innovation Platform Fund of universities in Hunan Province (Project No. 09K082), Project funded by China Postdoctoral Science Foundation (Project No. 2014M550418), and Open Project Program of State Key Laboratory of Chemo/Biosensing and Chemometrics (Project No. 2013008).

REFERENCES

- Han, M. Y.; Gao, X. H.; Su, J. Z.; Nie, S. *Nat. Biotechnol.* **2001**, *19*, 631.
- Hu, M.; Yan, J.; He, Y.; Lu, H.; Weng, L.; Song, S.; Fan, C.; Wang, L. *ACS Nano* **2010**, *4*, 488.
- Chen, X. L.; Estevez, M. C.; Zhu, Z.; Huang, Y. F.; Chen, Y.; Wang, L.; Tan, W. H. *Anal. Chem.* **2009**, *81*, 7009.
- Wang, L.; Zhao, W.; O'Donoghue, M. B.; Tan, W. *Bioconjugate Chem.* **2007**, *18*, 297.
- Frigoli, M.; Ouadahi, K.; Larpent, C. *Chem. Eur. J.* **2009**, *15*, 8319.
- Ner, Y.; Grote, J. G.; Stuart, J. A.; Sotzing, G. A. *Angew. Chem. Int. Ed.* **2009**, *48*, 5134.
- Gao, X. H.; Cui, Y. Y.; Levenson, R. M.; Chung, L. W. K.; Nie, S. M. *Nat. Biotechnol.* **2004**, *22*, 969.
- Zhang, Q.; Atay, T.; Tischler, J. R.; Bradley, M. S.; Bulovic, V.; Nurmikko, A. V. *Nat. Nanotechnol.* **2007**, *2*, 555.
- Kosaka, N.; Ogawa, M.; Sato, N.; Choyke, P. L.; Kobayashi, H. *J. Invest. Dermatol.* **2009**, *129*, 2818.
- Lin, S.; Xie, X.; Patel, M. R.; Yang, Y.-H.; Li, Z.; Cao, F.; Gheysens, O.; Zhang, Y.; Gambhir, S. S.; Rao, J. H.; Wu, J. C. *BMC Biotechnology* **2007**, *7*, 67.
- Chen, N.; He, Y.; Su, Y.; Li, X.; Huang, Q.; Wang, H.; Zhang, X.; Tai, R.; Fan, C. *Biomaterials* **2012**, *33*, 1238.
- Lee, S. F.; Osborne, M. A. *ChemPhysChem* **2009**, *10*, 2174.
- Wang, L.; Tan, W. H. *Nano Lett.* **2006**, *6*, 84.
- Wagh, A.; Jyoti, F.; Mallik, S.; Qian, S.; Leclerc, E.; Law, B. *Small* **2013**, *9*, 2129.
- Sauer, R.; Turshatov, A.; Balushev, S.; Landfester, K. *Macromolecules* **2012**, *45*, 3787.
- Zhang, J.; Wang, L. H.; Zhang, H.; Boey, F.; Song, S. P.; Fan, C. H. *Small* **2010**, *6*, 201.
- Li, C. H.; Zhang, Y. X.; Hu, J. M.; Cheng, J. J.; Liu, S. Y. *Angew. Chem. Int. Ed.* **2010**, *49*, 5120.

18. Chen, J.; Zhang, P. S.; Fang, G.; Yi, P. G.; Zeng, F.; Wu, S. *Z. J. Phys. Chem. B* **2012**, *116*, 4354.
19. Wan, X. J.; Liu, S. Y. *J. Mater. Chem.* **2011**, *21*, 10321.
20. Feng, X. L.; Yang, G. M.; Liu, L. B.; Lv, F. T.; Yang, Q.; Wang, S.; Zhu, D. B. *Adv. Mater.* **2012**, *24*, 637.
21. Li, Z. Q.; Zhang, Y.; Jiang, S. *Adv. Mater.* **2008**, *20*, 4765.
22. Song, J. Z.; Yang, Q.; Lv, F. T.; Liu, L. B.; Wang, S. *ACS Appl. Mater. Inter.* **2012**, *4*, 2885.
23. Rong, Y.; Wu, C. F.; Yu, J. B.; Zhang, X. J.; Ye, F. M.; Zeigler, M.; Gallina, M. E.; Wu, I. C.; Zhang, Y.; Chan, Y. H.; Sun, W.; Uvdal, K.; Chiu, D. T. *ACS Nano* **2013**, *7*, 376.
24. Pu, K. Y.; Li, K.; Liu, B. *Chem. Mater.* **2010**, *22*, 6736.
25. Wu, C. F.; Zheng, Y. L.; Szymanski, C.; McNeill, J. J. *Phys. Chem. C* **2008**, *112*, 1772.
26. Saleh, S. M.; Muller, R.; Mader, H. S.; Duerkop, A.; Wolfbeis, O. S. *Anal. Bioanal. Chem.* **2010**, *398*, 1615.
27. Fukui, Y.; Ozawa, Y.; Fujimoto, K. *J. Mater. Chem. C* **2013**, *1*, 1231.
28. Liu, J. Z.; Zhong, Y. C.; Lam, J. W. Y.; Lu, P.; Hong, Y. N.; Yu, Y.; Yue, Y. N.; Faisal, M.; Sung, H. H. Y.; Williams, I. D.; Wong, K. S.; Tang, B. Z. *Macromolecules* **2010**, *43*, 4921.
29. Wu, C.; Bull, B.; Szymanski, C.; Christensen, K.; McNeill, J. *ACS Nano* **2008**, *2*, 2415.
30. Xu, J. Q.; Liang, J. L.; Li, J.; Yang, W. S. *Langmuir* **2010**, *26*, 15722.
31. Qiao, Z. A.; Wang, Y. F.; Gao, Y.; Li, H. W.; Dai, T. Y.; Liu, Y. L.; Huo, Q. S. *Chem. Commun.* **2010**, *46*, 8812.
32. Qian, H. S.; Li, Z. Q.; Zhang, Y. *Nanotechnology* **2008**, *19*, 255601.
33. Pecher, J.; Huber, J.; Winterhalder, M.; Zumbusch, A.; Mecking, S. *Biomacromolecules* **2010**, *11*, 2776.
34. Cao, Y. C.; Wang, Z.; Wang, H. Q.; Wang, J. H.; Hua, X. F.; Jin, X.; Yang, L.; Huang, Z. L.; Liu, M. X.; Zhao, Y. D. *J. Nanosci. Nanotechnol.* **2009**, *9*, 1778.
35. Sachdev, A.; Matai, I.; Kumar, S. U.; Bhushan, B.; Dubey, P.; Gopinath, P. *RSC Adv.* **2013**, *3*, 16958.
36. Chen, J.; Zeng, F.; Wu, S. Z.; Su, J.; Tong, Z. *Small* **2009**, *5*, 970.
37. Antonietti, M.; Landfester, K. *Prog. Polym. Sci.* **2002**, *27*, 689.
38. Frochot, C.; Mascherin, M.; Haumont, A.; Viriot, M. L.; Marie, E. *J. Appl. Polym. Sci.* **2011**, *119*, 219.
39. Ando, K.; Kawaguchi, H. *J. Colloid Interface Sci.* **2005**, *285*, 619.
40. Grabchev, I.; Konstantinova, T. *Dyes. Pigm.* **1997**, *33*, 197.
41. Konstantinova, T. N.; Meallier, P.; Grabchev, I. *Dyes. Pigm.* **1993**, *22*, 191.
42. Onoda, M.; Uchiyama, S.; Santa, T.; Imai, K. *Anal. Chem.* **2002**, *74*, 4089.
43. Briggs, M. S. J.; Bruce, I.; Miller, J. N.; Moody, C. J.; Simmonds, A. C.; Swann, E. *J. Chem. Soc. Perkin. Trans. 1.* **1997**, 1051.
44. Valeur, B. In *Molecular Fluorescence: Principles and Applications*; Wiley-VCH: New York, Weinheim, **2002**.
45. Lakowicz, J. R. In *Principles of Fluorescence Spectroscopy*; Kluwer Academic: New York, **1999**.
46. Grazon, C.; Rieger, J.; Meallet-Renault, R.; Charleux, B.; Clavier, G. *Macromolecules* **2013**, *46*, 5167.
47. Resch-Genger, U.; Grabolle, M.; Cavaliere-Jaricot, S.; Nitschke, R.; Nann, T. *Nat. Methods* **2008**, *5*, 763.
48. Sun, G. R.; Berezin, M. Y.; Fan, J. D.; Lee, H.; Ma, J.; Zhang, K.; Wooley, K. L.; Achilefu, S. *Nanoscale* **2010**, *2*, 548.